

Blue Turns to Gray: Paleogenomic Insights into the Evolutionary History and Extinction of the Blue Antelope (*Hippotragus leucophaeus*)

Elisabeth Hempel ,^{*,1,2} Faysal Bibi ,² J. Tyler Faith ,^{3,4,5} Klaus-Peter Koepfli ,^{6,7} Achim M. Klittich,¹ David A. Duchêne ,^{8,9} James S. Brink,^{†,10,11} Daniela C. Kalthoff ,¹² Love Dalén ,^{13,14,15} Michael Hofreiter ,^{‡,1} and Michael V. Westbury ,^{‡,8}

¹Evolutionary Adaptive Genomics, Institute for Biochemistry and Biology, Department of Mathematics and Natural Sciences, University of Potsdam, Karl-Liebknecht-Str. 24-25, 14476 Potsdam, Germany

²Museum für Naturkunde, Leibniz Institute for Evolution and Biodiversity Science, Invalidenstraße 43, 10115 Berlin, Germany

³Natural History Museum of Utah, University of Utah, 301 Wakara Way, Salt Lake City, UT 84108

⁴Department of Anthropology, University of Utah, 260 South Central Campus Drive, Salt Lake City, UT 84112

⁵Origins Centre, University of the Witwatersrand, Johannesburg, Republic of South Africa

⁶Smithsonian-Mason School of Conservation, George Mason University, Front Royal, VA 22630

⁷Center for Species Survival, Smithsonian's National Zoo and Conservation Biology Institute, Washington, DC, 20008, USA

⁸Globe Institute, University of Copenhagen, Øster Voldgade 5-7, Copenhagen, Denmark

⁹Centre for Evolutionary Hologenomics, University of Copenhagen, Copenhagen 1352, Denmark

¹⁰National Museum Bloemfontein, Florisbad Quaternary Research Station and Department, PO Box 266, Bloemfontein 9031, Republic of South Africa

¹¹Centre for Environmental Management, University of the Free State, PO Box 339, Bloemfontein 9300, Republic of South Africa

¹²Swedish Museum of Natural History, Department of Zoology, Box 50007, 10405 Stockholm, Sweden

¹³Swedish Museum of Natural History, Department of Bioinformatics and Genetics, Box 50007, 10405 Stockholm, Sweden

¹⁴Centre for Palaeogenetics, Svante Arrhenius väg 20c, 10691 Stockholm, Sweden

¹⁵Department of Zoology, Stockholm University, 10691 Stockholm, Sweden

[†]Deceased.

[‡]These authors shared senior authorship.

***Corresponding author:** E-mail: Hempel.Elisabeth@posteo.org.

Associate editor: Jian Lu

Abstract

The blue antelope (*Hippotragus leucophaeus*) is the only large African mammal species to have become extinct in historical times, yet no nuclear genomic information is available for this species. A recent study showed that many alleged blue antelope museum specimens are either roan (*Hippotragus equinus*) or sable (*Hippotragus niger*) antelopes, further reducing the possibilities for obtaining genomic information for this extinct species. While the blue antelope has a rich fossil record from South Africa, climatic conditions in the region are generally unfavorable to the preservation of ancient DNA. Nevertheless, we recovered two blue antelope draft genomes, one at 3.4× mean coverage from a historical specimen (~200 years old) and one at 2.1× mean coverage from a fossil specimen dating to 9,800–9,300 cal years BP, making it currently the oldest paleogenome from Africa. Phylogenomic analyses show that blue and sable antelope are sister species, confirming previous mitogenomic results, and demonstrate ancient gene flow from roan into blue antelope. We show that blue antelope genomic diversity was much lower than in roan and sable antelope, indicative of a low population size since at least the early Holocene. This supports observations from the fossil record documenting major decreases in the abundance of blue antelope after the Pleistocene–Holocene transition. Finally, the persistence of this species throughout the Holocene despite low population size suggests that colonial-era human impact was likely the decisive factor in the blue antelope's extinction.

Key words: ancient DNA, diversity, extinction, Holocene, paleogenome, South Africa.

Introduction

Earth is currently undergoing a major biodiversity crisis that is a direct result of human activities (Ceballos et al. 2015). The consequences for many species include considerable reductions in population size and associated losses of genetic diversity that can lead to reduced fitness and adaptability. Today, through the continuing development of next generation sequencing technologies and advancement of ancient DNA (aDNA) techniques, it is feasible to retrieve genomic information from extinct and non-model organism species (Westbury et al. 2020; Barlow et al. 2021; Sánchez-Barreiro et al. 2021), thereby facilitating inferences about threats facing many present-day species. One especially powerful use of these genomes is to reconstruct the evolutionary history of species in relation to environmental change and human impacts. In this regard, Africa is hugely understudied, likely due to its environmental conditions, with high temperatures being detrimental to DNA preservation (Smith et al. 2001; Bollongino et al. 2008; Hofreiter et al. 2015). To date, most aDNA studies on African samples have been restricted to DNA enrichment approaches and focused on human remains (Skoglund et al. 2017; Vicente and Schlebusch 2020; Lipson et al. 2022), with very few investigating other fossil fauna (e.g., Mathieson et al. 2020).

One species that likely fell victim to human impacts during the beginning of the current biodiversity crisis is the blue antelope, *Hippotragus leucophaeus* (Pallas, 1766). The blue antelope belongs to the bovid tribe Hippotragini, which comprises the extant genera *Hippotragus*, *Oryx*, and *Addax*. It went extinct ~1800 AD (Lichtenstein 1811, 1814) and therefore represents the first — and so far only — historical extinction of a large African mammal species (Harper 1945), though several subspecies have become extinct in the last few hundred years (e.g., quagga [*Equus quagga quagga*], bubal hartebeest [*Alcelaphus buselaphus buselaphus*], and Cape wart-hog [*Phacochoerus aethiopicus aethiopicus*]; d'Huart and Grubb 2001; Hack et al. 2008; IUCN SSC Antelope Specialist Group 2017). The blue antelope had a distinct white patch in front of the eyes (Pallas 1767), and its pelt was perceived as bluish while alive (Lichtenstein 1814; von Schreber and Goldfuß 1836) — perhaps similar to the blue wildebeest (*Connochaetes taurinus*) or the nilgai (*Boselaphus tragocamelus*) (Mohr 1967) — turning grayish post-mortem (Lichtenstein 1814; von Schreber and Goldfuß 1836) (fig. 1B). Like its extant relatives, the blue antelope was a grazer (Mohr 1967; Klein 1974, 1987). Historically, the blue antelope was endemic to a very small area (~4,300 km²) between Swellendam, Caledon, and Bredasdorp in South Africa (Skead 1980; Kerley et al. 2009). However, its Quaternary fossil record demonstrates a broader prehistoric range (fig. 1A), with fossil occurrences throughout the Cape Floristic Region and extending into the highlands of Lesotho (Klein 1974; Plug 1997; Faith and Thompson 2013; Avery 2019). Blue antelopes are particularly ubiquitous and abundant in

Pleistocene archaeological and paleontological assemblages from South Africa's Western Cape Province, contracting in range and abundance at the onset of the Holocene (Faith 2011). Its occurrence in both late Pleistocene and Holocene archaeological sites implies a long history of human predation on blue antelope that spans at least the past ~100,000 years (e.g., Klein 1976; Faith 2013), with evidence from Elandsfontein indicating that hominins and blue antelope have overlapped since the mid-Pleistocene (~1 Ma to 600 ka) (Klein et al. 2007). The blue antelope's extinction is hypothesized to have been the result of several, mostly recent anthropogenic drivers, including landscape transformation (Faith and Thompson 2013), overhunting by European colonists (FitzSimons 1920; Harper 1945), competition with and habitat deterioration by livestock (Klein 1974, 1987), and disruption of migratory pathways in prehistoric and colonial times (Faith and Thompson 2013). Additionally, the potentially detrimental role of stochastic processes in a small population has also been considered (Kerley et al. 2009). Unfortunately, due to its early demise, our primary sources of knowledge of the blue antelope's ecology and evolutionary history have so far been limited to information from the fossil record (Klein 1974, 1987; Faith 2011; Faith and Thompson 2013) and historical mitochondrial data (Robinson et al. 1996; Themudo and Campos 2018; Hempel, Bibi, et al. 2021).

The relationships among the three *Hippotragus* species, the roan (*H. equinus*), the sable (*H. niger*) and the blue antelope, have so far only been investigated using morphological evidence (Vrba and Gatesy 1994) and mitochondrial sequences (Robinson et al. 1996; Themudo and Campos 2018; Hempel, Bibi, et al. 2021), leaving their phylogeny unresolved at the nuclear genome level. Considering that mitochondrial DNA data can present an incomplete picture of the evolutionary history of a species and can be confounded by past gene flow events (e.g., Larsen et al. 2010; Reich et al. 2010; Edwards et al. 2011; Hailer et al. 2012; Westbury et al. 2020; Liu et al. 2021), nuclear data are necessary to conclusively resolve phylogenetic relationships.

Here, we present the nuclear genome of a ~200-year-old blue antelope specimen as well as a paleogenome from an early Holocene fossil specimen (9,800–9,300 cal years BP) recovered from Klein's 1971–1972 excavation of archaeological deposits at Nelson Bay Cave, located on the Robberg Peninsula at Plettenberg Bay (Klein 1972; see Materials and Methods for further details). To our knowledge, the paleogenome extracted from this early Holocene fossil specimen (NBC RB4 D3) is currently the oldest paleogenome from Africa. Using these genomes, we investigate and date the phylogenomic relationships of the blue antelope and show that the blue antelope was more closely related to the sable than to the roan antelope, but with detectable past gene flow between the roan and the blue antelope. Furthermore, we demonstrate that the blue antelope had very low diversity

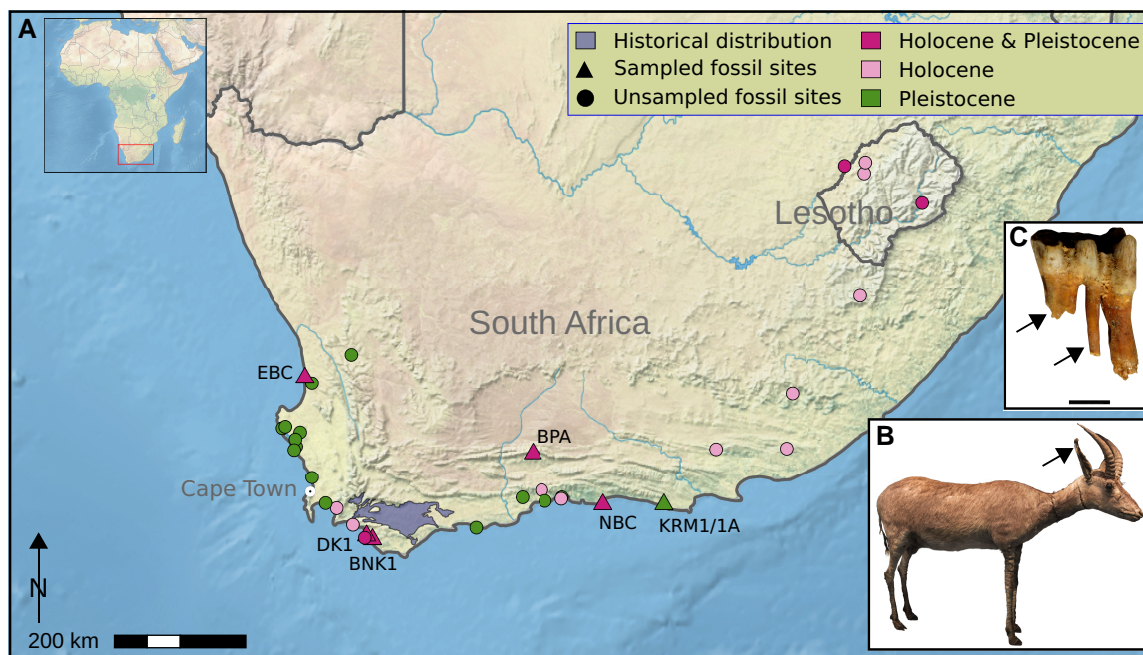


FIG. 1. Blue antelope distribution and specimens. (A) Historical distribution (light purple at the southern tip) and Quaternary fossil occurrences of blue antelope (Skead 1980; Kerley et al. 2009; modified from Avery 2019). Fossil sites: EBC = Elands Bay Cave, DK1 = Die Kelders Cave 1, BNK1 = Byneskranskop 1, BPA = Boomplaas Cave, NBC = Nelson Bay Cave, KRM1/1A = Klasies River Mouth 1/1A (base map: <https://www.natureearthdata.com>, prepared in QGIS v2.18 [<https://qgis.org>]). (B) Historical mounted skin of a young male blue antelope (*Hippotragus leucophaeus*) from the Swedish Museum of Natural History, Stockholm, Sweden (NRM 590107); arrow indicates area sampled for aDNA extraction. (C) Fossil lower left deciduous fourth premolar (NBC RB4 D3) of a blue antelope from Nelson Bay Cave (curated at Iziko Museums of South Africa, Cape Town, South Africa); scale is one centimeter; arrows indicate areas sampled for aDNA extraction. Photo credits: NBC RB4 D3: J.T. Faith, courtesy: Archaeology Unit, Iziko Museums of South Africa; NRM 590107: Hempel, Bibi, et al. (2021).

compared with its congeners, likely since at least the beginning of the Holocene.

Results

Sequencing Results

Using shotgun sequencing, we obtained both a nuclear and a mitochondrial genome from a fossil specimen from Nelson Bay Cave (NBC RB4 D3; Klein 1972, 1983) dating to 9,800–9,300 cal years BP (Loftus et al. 2016) at 2.14× and 234.67× mean coverages, respectively. In addition, we generated a nuclear genome of the ~200-year-old historical specimen NRM 590107 from the Swedish Museum of Natural History, Stockholm, Sweden, with a mean coverage of 3.44×. Details on read numbers and mapping statistics can be found in [supplementary tables S2 and S3, Supplementary Material](#) online. MapDamage v2.2.0 (Jónsson et al. 2013) analysis of DNA sequences obtained from the NBC RB4 D3 specimen showed typical patterns of damage (caused by cytosine deamination) for an aDNA sample of its age ([supplementary figs. S1A and S1B, Supplementary Material](#) online). The same was true for NRM 590107, but in addition, this sample also showed an elevated level of guanine to thymine transversions ([supplementary figs. S2A and S2B, Supplementary Material](#) online). This pattern could originate from a hydrogen peroxide treatment of the sample or any other

treatment causing oxidative damage, as oxidative DNA damage results in 8-hydroxy-guanine (Kvam and Tyrrell 1997; Nohmi et al. 2005) and this modified base pair with adenine, resulting in guanidine to thymine changes. However, such a treatment has not been documented for the individual from the Swedish Museum of Natural History.

Phylogenetic Relationships

Nuclear genome phylogenetic analyses using neighbor joining and 20 kb sliding window trees under the multispecies coalescent supported the monophyly of all three *Hippotragus* species and showed that the blue antelope is more closely related to the sable than to the roan antelope ([fig. 2, supplementary fig. S3, Supplementary Material](#) online). Out of the 20 kb sliding window trees, 50.46% were concordant with the species tree, which is strong support in the case of an unrooted phylogenetic quartet ([supplementary table S9, Supplementary Material](#) online). As there are only three possible resolutions of an unrooted quartet, the other resolutions had to share the remaining 50% (roan + blue antelope as sister = 29.78% and roan + sable antelope as sister = 19.75%). Therefore, this result shows strong support in the data for this particular resolution. A principal component analysis ([supplementary fig. S4, Supplementary Material](#) online) confirmed that both blue antelope samples cluster tightly together and are more closely related to each other than they are to

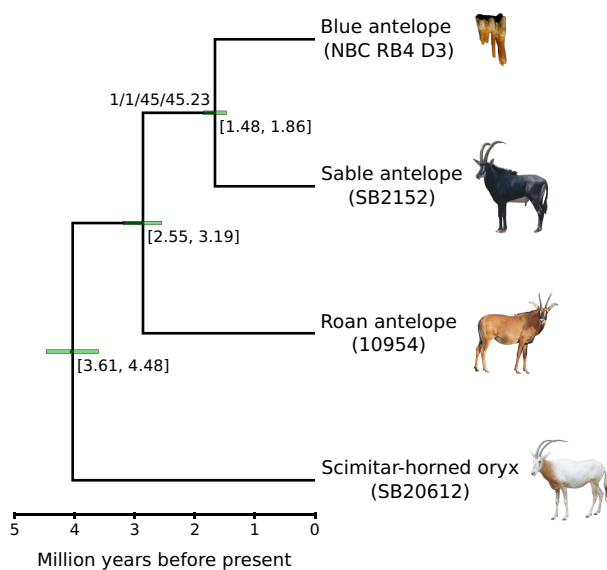


Fig. 2. Phylogenetic analysis. Dated phylogenetic tree computed using nuclear and mitochondrial data from the three *Hippotragus* species. The tree topology was inferred using a data set that excluded transition-only sites, under the multispecies coalescent model using ASTRAL v4.10 (Rabiee et al. 2019), whereas the timescale was inferred using MCMCTree v4.9 (dos Reis and Yang 2011). Node annotations below age credibility interval bars show the respective credibility interval's range in Ma, whereas the branch label shows support values (bootstrap, local posterior probability, gene concordance factor, and site-concordance factor). Branch support is calculated on an unrooted tree; in this case with four taxa, so the support is for the separation between two pairs of taxa as represented by that single internal branch. The scimitar-horned oryx was used as outgroup (Humble et al. 2020). Roan and sable antelope raw data are from Gonçalves et al. (2021) and Koepfli et al. (2019). Photo credits: NBC RB4 D3: J.T. Faith, courtesy: Archaeology Unit, Iziko Museums of South Africa; roan antelope: Charles J. Sharp, wikipedia commons, CC-BY 4.0; sable antelope: Paulmaz, wikipedia commons, CC-BY 3.0; scimitar-horned oryx: E. Hempel.

any other individual in the data set. Bayesian molecular dating using MCMCTree yielded a median posterior age of the split between the blue and sable antelope of 1.67 Ma, with a 95% credibility interval ranging between 1.48 and 1.86 Ma. The split between the roan and sable/blue antelope had a median of 2.86 Ma and a 95% credibility interval ranging between 2.55 and 3.19 Ma (fig. 2).

The mitochondrial genome maximum-likelihood phylogeny was congruent with the nuclear phylogeny (fig. 2, supplementary figs. S3 and S6A, Supplementary Material online). The mitochondrial phylogeny using transversions only (binary format) also yielded an identical topology with respect to the grouping of the three species (supplementary fig. S6B, Supplementary Material online). The split between the blue and sable antelope mitochondrial genomes was dated to a median posterior age of 2.29 Ma (95% credibility interval: 1.63–2.93 Ma) by MCMCTree. The median of the split between roan and sable/blue antelope was 3.49 Ma (95% credibility interval: 2.77–4.25 Ma; supplementary fig. S7, Supplementary Material online). 51.97% of the informative sites were concordant with the species tree.

Gene Flow

Both blue antelope individuals showed significantly higher levels of shared derived alleles with the roan antelope compared with the sable antelope, suggestive of gene flow between blue and roan antelope (fig. 3A, supplementary table S7, Supplementary Material online). Sliding window phylogenetic tree analyses also suggested gene flow between blue and roan antelope, as more windows contained phylogenies with a closer affinity between roan and blue antelope than between roan and sable antelope (fig. 3C, supplementary table S8 and S9, Supplementary Material online). Moreover, by comparing multiple individuals per species, the sliding window analysis showed that gene flow between roan and blue antelope occurred after the split of blue and sable antelope but before the split of the most recent common ancestors of all roan and also the two blue antelope individuals analyzed in our study.

To determine the directionality of the gene flow, we utilized the branch lengths between roan and sable antelope in window trees where the roan and blue antelope form sister lineages. It was expected that in case of gene flow from roan into blue antelope the branch lengths between roan and sable antelope would be in agreement with the species tree topology, whereas gene flow from blue into roan antelope would lead to a higher similarity between roan and sable antelope and thereby to a shorter branch length compared with the species tree topology (fig. 4A). The sliding window analysis with branch length calculations showed that the branch lengths of roan and sable antelope were similar for the inferred species tree topology and the alternative topology placing blue and roan antelope as sister lineages. Assuming that the most frequently found topology is the species tree topology, the next most frequent topology presumably results from both incomplete lineage sorting and/or gene flow. A bimodal distribution would have been expected if there had been any occurrence of gene flow from the blue into the roan antelope. One mode would reflect the relatively ancient species divergence between the roan and the sable antelope, whereas the other mode would reflect the more recent divergence between the introgressed blue antelope loci and the sable antelope. As the distributions of branch lengths between roan and sable antelope were unimodal and approximately equal between windows resulting in the species tree topology and the second most frequent topology, the direction of gene flow was most likely from the roan into the blue antelope (fig. 4B).

Nuclear and Mitochondrial Diversity

Calling heterozygous positions to estimate the nuclear genomic diversity of the two low coverage genomes was not a reliable option. Therefore, we estimated diversity through an alternative measure. By uniquely evaluating each substitution type, we confirmed elevated cytosine to thymine and guanine to thymine levels found via mapDamage (supplementary figs. S1 and S2, Supplementary Material online). After removing substitutions that could have been caused by DNA damage, our results show that pairwise differences are related to

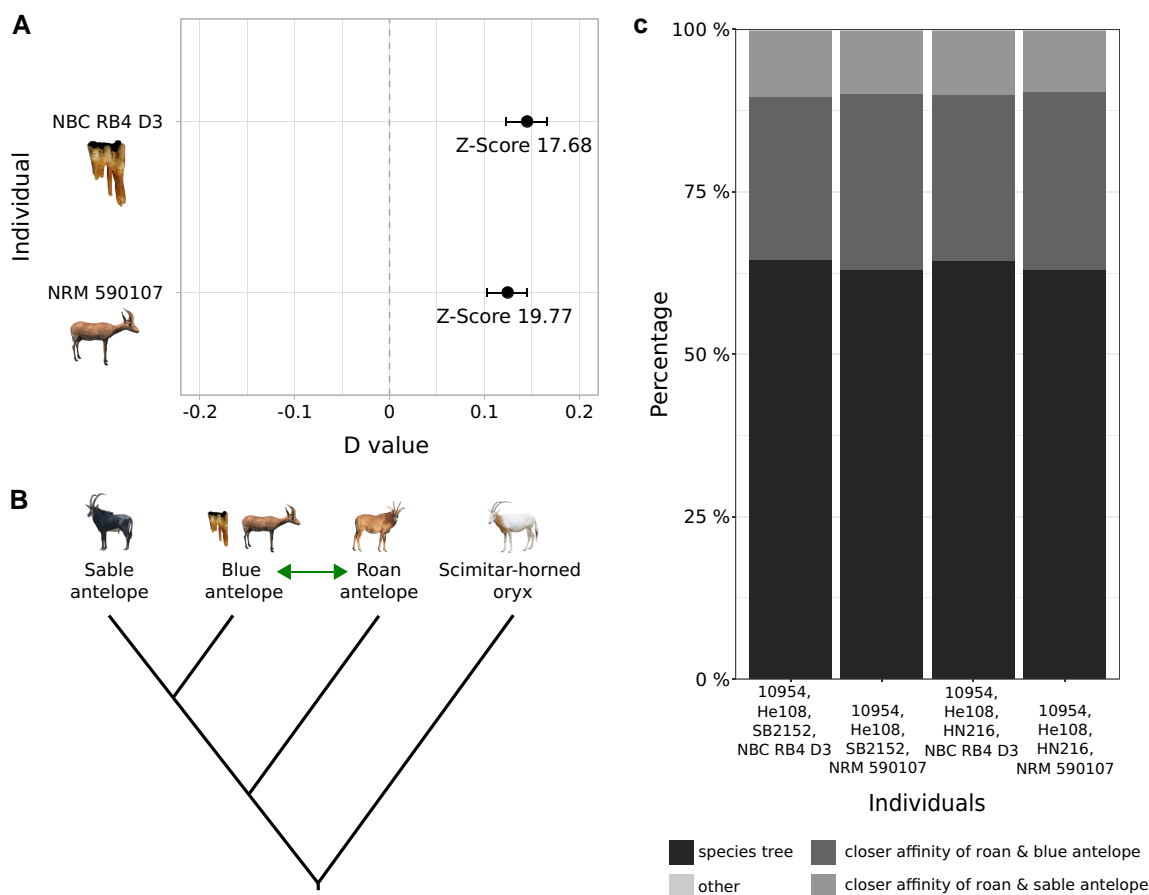


Fig. 3. Gene flow analyses for the three *Hippotragus* species. (A) D values and Z-scores of D statistics for the fossil (NBC RB4 D3) and historical (NRM 590107) blue antelope specimens showing significant gene flow between blue and roan antelope demonstrated by positive D values; analysis performed with Dstat (transversions only version, <https://github.com/jacahill/Admixture>). A $Z\text{-score} > |3|$ is regarded as significant. (B) Tested topology for D statistics according to the 20 kb sliding window multispecies coalescent and the neighbor joining phylogenies (fig. 2 and supplementary fig. S3, Supplementary Material online) with blue antelope in position 2. The green double arrow indicates gene flow between blue and roan antelope with unknown directionality. (C) Percentages of tree topologies in the 100 kb sliding window tree analysis. In every combination, more windows show a closer affinity between roan and blue antelope than between roan and sable antelope. Topologies in category “other” were so rare that they are not visible in the figure. Roan antelope: 10954, He108 (Gonçalves et al. 2021); sable antelope: SB2152, HN216 (Koepfli et al. 2019); blue antelope: NBC RB4 D3, NRM 590107. Photo credits: NBC RB4 D3: J.T. Faith, courtesy: Archaeology Unit, Iziko Museums of South Africa; NRM 590107: Hempel, Bibi, et al. (2021); roan antelope: Charles J. Sharp, wikipedia commons, CC-BY 4.0; sable antelope: Paulmaz, wikipedia commons, CC-BY 3.0; scimitar-horned oryx: E. Hempel.

mean heterozygosity in roan and sable antelope. Therefore, we concluded that pairwise differences could be used to reliably estimate species-wide nuclear diversity even when using low coverage genomes (fig. 5, supplementary tables S10–12 and S16, Supplementary Material online).

Pairwise difference estimates showed that the blue antelope had much lower nuclear diversity than the roan and sable antelope (fig. 5). The roan antelope showed the highest nuclear diversity among the three *Hippotragus* species, with the sable antelope showing values that were lower than the roan antelopes’ but still much higher than those of the blue antelope. Comparing subsampled and not subsampled input data for the pairwise difference estimates showed that coverage can have an influence, but not to the extent that it could result in the substantially reduced nuclear diversity of the blue antelope observed relative to the other species (supplementary fig. S5 and tables S13–S15, Supplementary Material online).

To estimate the mitochondrial genome diversity of the blue antelope, we generated two haplotype networks, one using complete and the other using partial mitochondrial genomes. The removal of all ambiguities/missing data resulted in an alignment length of 16,492 bp for the complete mitochondrial alignment and 6,300 bp for the partial mitochondrial alignment. We found 15 segregating sites and a nucleotide diversity of 0.00061 in the alignment with complete mitochondrial genomes (supplementary fig. S8A, Supplementary Material online), and 10 segregating sites and a very similar nucleotide diversity of 0.00067 for the alignment with partial mitochondrial genomes (supplementary fig. S8B, Supplementary Material online).

Discussion

Using aDNA techniques, we sequenced the first nuclear genomes of the blue antelope to study its evolutionary

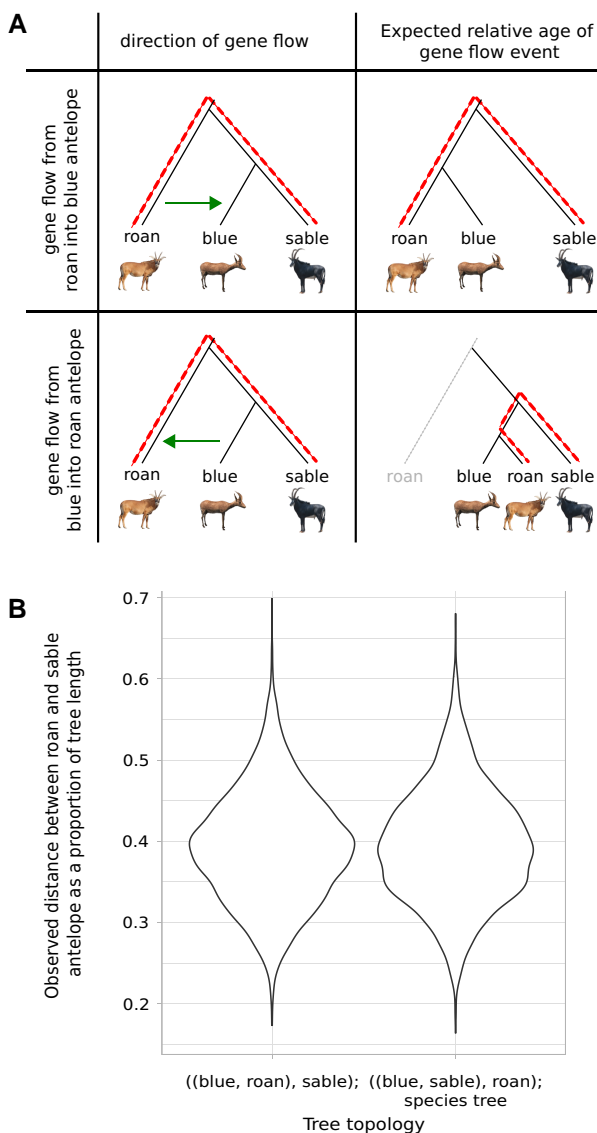


Fig. 4. Gene flow direction analysis. (A) Expected outcome of changes in genetic distances for gene flow (green arrow) from roan into blue antelope and blue into roan antelope. Dashed red lines illustrate the expected distances between roan and sable antelope. (B) Genetic distances between roan and sable antelope as a proportion of the tree length performed with WindowTrees v1.0.0 (<https://github.com/achimklittich/WindowTrees>). Photo credits: see fig. 3.

history and genetic diversity, and to provide insights into the only historical extinction of a large African mammal species to date. The retrieval of aDNA from African fossils is a challenging task because of prevailing environmental conditions, namely high temperatures, which facilitate DNA degradation (Smith et al. 2001; Bollongino et al. 2008; Hofreiter et al. 2015). For this reason, few studies have succeeded in recovering aDNA from Africa, and the few exceptions were mainly focused on humans and used genomic enrichment approaches (Vicente and Schlebusch 2020; Lipson et al. 2022). Nonetheless, despite such challenges, we were able to successfully sequence a sample that, with an age of 9,800–9,300 cal years BP,

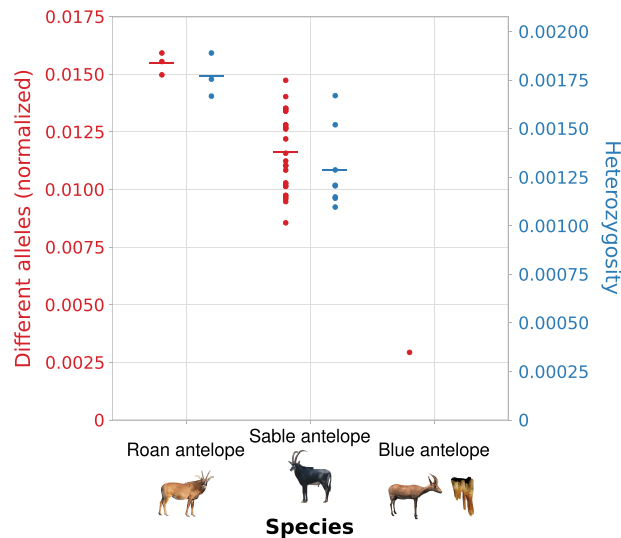


Fig. 5. Nuclear diversity analysis. Species-wide nuclear diversity of the three *Hippotragus* species computed from pairwise comparisons (data normalized by dividing by the number of sites used in the analysis — 2,243,953 sites; genomes for heterozygosity subsampled to 4.26× mean coverage, the lowest mean coverage in the roan/sable antelope data set). Each dot represents a pairwise comparison. Lines represent means. Heterozygosity was not estimated for the blue antelope due to low coverage and aDNA damage. Photo credits: see fig. 3.

currently represents the oldest paleogenome from Africa. Our success demonstrates that paleogenomes can be recovered successfully from southern African sites, setting the stage for future genomic studies from this area. It is worth noting that our fossil specimen originates from cave deposits in South Africa's southern Cape region, which should have higher potential for aDNA recovery than, for example, fossils from fluvial sediments in tropical Africa (Hofreiter et al. 2015).

Our finding that the blue antelope is more closely related to the sable than to the roan antelope on a nuclear level confirms results from studies based on mitochondrial genome sequences (Robinson et al. 1996; Themudo and Campos 2018; Hempel, Bibi, et al. 2021) and contradicts phylogenies relying on morphological evidence, which placed roan and blue antelope as sister species (Vrba and Gatesy 1994). As mitochondrial DNA represents a single genetic locus, it was not certain if the mitochondrial phylogeny alone could reliably settle the question of the relationships among the three *Hippotragus* species, as it could have been biased by introgression or incomplete lineage sorting as has been shown in other species (e.g., Barlow et al. 2018; Rakotoarivelo et al. 2019; Westbury et al. 2020). However, our phylogenomic results confirm the relationships among the recent species of *Hippotragus* using nuclear data, although they place the timing of the split between roan and sable/blue antelope as well as the split between sable and blue antelope younger than estimates from mitochondrial genomes (supplementary fig. S7, Supplementary Material online, this study; Themudo and Campos 2018). We consider

the nuclear data set to be a better representation of the divergence time as it is far larger than the mitochondrial data set, and is therefore less susceptible to stochastic error. Moreover, as we found gene flow to have occurred in our *Hippotragus* data set, a more recent divergence time on the nuclear level could also be the result of gene flow between the roan and ancestor of the blue/sable antelope as well as between the blue and sable antelope after their initial divergences, leading to overall shorter branch lengths and younger estimates compared with the mitochondrial genomes, especially when the gene flow was male driven. The estimated divergence age of ~1.67 Ma between the sable and blue antelope strongly suggests that the blue antelope represents a separate species, which resolves the long-going discussion on whether the blue antelope was a distinct species or not (Smith 1849; Kohl 1886; Mohr 1967).

Both blue antelope specimens showed significantly higher levels of gene flow with the roan antelope relative to that between the roan and the sable antelope. This may look surprising at first, as the extant and historical populations of the roan and the sable antelope overlap considerably. However, the ranges of the roan and the blue antelope also overlapped in the southern Cape region during the late Pleistocene and Holocene (fig. 6; Klein 1972; Faith 2012; Avery 2019). Interspecific gene flow is known to be more likely when population size is low as the chances of finding a conspecific mating partner are reduced (Hubbs principle; Hubbs 1955; Jansson et al. 2007; Crossman et al. 2016; Vaz Pinto et al. 2016). Although we were unable to directly date the gene flow event(s), we could show that gene flow occurred after the split of blue and sable antelope but before the last common ancestors of the roan antelope individuals included in this study. While we did not detect evidence for more recent interspecific gene flow, it may have been biologically possible as roan and blue antelope have the same evolutionary distance as roan and sable antelope, which are likely still able to produce viable offspring (Robinson and Harley 1995; Vaz Pinto et al. 2016).

The genomic evidence for low diversity and therefore potentially low population sizes since the early Holocene confirms observations derived from the fossil record. Fossil evidence from southern Africa suggests that the blue antelope was both widespread and abundant during the last glacial period (~115 to 11.7 ka) (Klein 1987; Faith 2011). It became increasingly rare in the fossil record following the Pleistocene–Holocene transition (Faith 2011), with the long stratified sequence at Nelson Bay Cave — from where our fossil specimen originates — demonstrating that it remained a rare component of the large mammal community throughout the Holocene (Klein 1983). The onset of the population decline of the blue antelope near the Pleistocene–Holocene transition broadly coincides with the extinction of several other large-bodied grazers in southern Africa, including Cape zebra (*Equus capensis*), long-horn buffalo (*Synacerus antiquus*), and giant wildebeest (*Megalotragus*

priscus), among others. These losses have been linked at least in part to declines in the availability and year-round productivity of grassy forage (Klein 1980; Brink and Lee-Thorp 1992; Faith 2014). This is particularly evident in the Cape Floristic Region, where grassy habitats diminished in conjunction with a rise in sea levels and drowning of the Palaeo-Agulhas Plain that would have contributed to dramatic habitat loss, disruption of possible migratory routes, and fragmentation of species ranges (Dingle and Rogers 1972; Klein 1983; van Andel 1989; Fisher et al. 2010; Compton 2011; Faith and Behrensmeyer 2013; Faith and Thompson 2013; Copeland et al. 2016; Venter et al. 2020). Rare Holocene occurrences of the blue antelope in the southwestern Cape (Klein and Cruz-Uribe 2016), the southern Cape (Klein 1983), and in the interior (Opperman 1987; Plug 1997), likely represent disjunct populations due to lack of dispersal corridors around the Cape Fold Mountains when sea levels were high (Compton 2011; Faith and Behrensmeyer 2013; Faith and Thompson 2013).

It appears that by the onset of historical times, the blue antelope had become restricted to the southern Cape (Klein 1983, but see Loubser et al. 1990), an area that provides limited foraging opportunities for large-bodied grazers (Klein 1983; Kerley et al. 2009; Faith and Behrensmeyer 2013; Cawthra et al. 2015, 2020). Thus, the environmental changes that marked the transition from the Pleistocene to the Holocene are likely to have resulted in a geographically isolated and small population (Skead 1980; Kerley et al. 2009), which conforms with our finding of very low nuclear diversity compared with the two extant *Hippotragus* species that were and are more broadly distributed across southern Africa (figs. 5 and 6). Archaeological evidence suggests that prehistoric human populations increased in southern Africa beginning ~15,000 years ago (Deacon and Thackeray 1984; Wadley 1993), but whether this contributed to the low population size of blue antelope by the early Holocene (e.g., via increased predation pressure) is presently uncertain. Linking prehistoric human activities to the blue antelope and other large-bodied ungulates from the region will require a more detailed understanding of their population histories through time and in relation to paleoclimatic, paleoenvironmental, and archaeological records.

Low nuclear diversity, and likely low population size, have characterized the blue antelope at least since the early Holocene, raising the question of whether the blue antelope was doomed to extinction, or whether it could have survived in the absence of increased human impacts in historical times. As Kerley et al. (2009) pointed out, due to increased susceptibility to drift there might have been an accumulation of mildly deleterious mutations in the small remaining blue antelope population, which might have put the species on a slow path to extinction.

Our finding of low diversity since the early Holocene, suggests that low diversity was most likely the result of climatically induced habitat loss and fragmentation at the

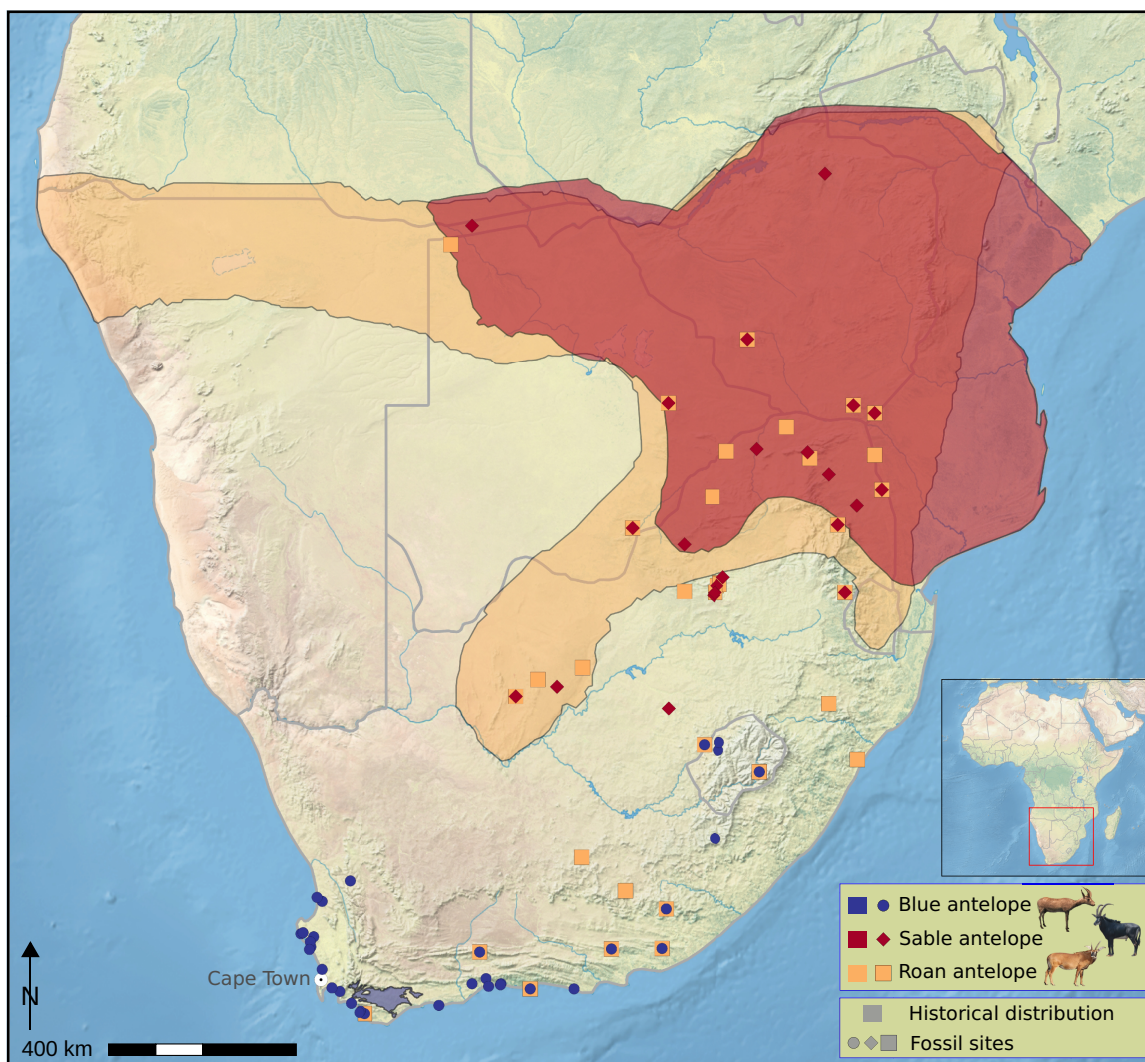


Fig. 6. Species distribution and fossil sites. Historical distribution and Holocene and Pleistocene fossil sites of blue, sable, and roan antelope in southern Africa. The distributions of the roan and sable antelope further north are not shown (base map: <https://www.naturalearthdata.com>, prepared in QGIS v2.18 (<https://qgis.org>; du Plessis 1969; Kerley et al. 2009; modified from Avery 2019). Photo credits: see fig. 3.

Pleistocene–Holocene transition, long before the introduction of livestock to the southern Cape (~2,000 years ago, Couto et al. 2021) or overhunting and landscape transformation during the colonial era. Generally, low diversity is associated with increased extinction risk (DeWoody et al. 2021; Kardos et al. 2021). However, the persistence of blue antelope for at least 10,000 years despite the possibility of continuously low diversity suggests that low diversity might not have impacted the survivability of the species, similar to other species in southern Africa (Westbury et al. 2018; Sánchez-Barreiro et al. 2021). Cycles of habitat restrictions through past changes in sea level and forage availability may have led to repeated declines in population size and genetic diversity. Continuously low population size may have enabled more efficient purging of highly deleterious mutations by exposing them more often in a homozygous state, meaning that low population size might be an adaptive advantage rather than a detriment (Xue et al. 2015; Dussex et al. 2021; Liu

et al. 2021). However, hunting with firearms and land transformation in the blue antelope's restricted habitat during the colonial era (FitzSimons 1920; Harper 1945; Kerley et al. 2003; Skead 2011; Faith and Thompson 2013) might have proved too much given this species' low population size, ultimately culminating in its extinction at the hands of humans.

In conclusion, our study shows that using genomic data from fossil specimens from Africa opens up new research possibilities to understand evolutionary dynamics. For the blue antelope, we found low diversity throughout the Holocene, confirming observations derived from the fossil record. In the future, it will be interesting to see if genomic data from Pleistocene specimens will continue to reflect the patterns seen in the fossil record. Our results suggest that humans in the colonial era caused the extinction of a species that was likely already vulnerable due to habitat loss and range fragmentation at least since the onset of the Holocene.

Materials and Methods

Samples

We obtained tooth root or bone samples from 25 blue antelope (*H. leucophaeus*) fossil specimens from Archaeology Unit, Iziko Museums of South Africa, Cape Town, South Africa, ranging between 71,000 and 5,000 cal years BP (supplementary table S1, Supplementary Material online) originating from six different fossil sites: Boomplaas Cave, Byneskranskop 1, Die Kelders Cave 1, Elands Bay Cave, Nelson Bay Cave and Klasies River Mouth 1/1A (fig. 1). Two samples were undated. Sample BNK1 O25/2 5.2 was radiocarbon-dated at the ¹⁴Chrono Centre, Queens University Belfast, Ireland, using CALIB REV 7.0.0 (Stuiver and Reimer 1993; supplementary table S1, Supplementary Material online). In addition, we used the single-stranded library of a historical sample from the Swedish Museum of Natural History in Stockholm, Sweden, from a previous study (Hempel, Bibi, et al. 2021).

The Nelson Bay Cave specimen (NBC RB4 D3) that yielded a paleogenome is a lower left deciduous premolar (dP₄). The strongly pinched lingual lobes and presence of basal pillars are consistent with *Hippotragus*, and its relatively small size relative to a handful of larger *Hippotragus* dP₄s from the site support attribution to *H. leucophaeus* (see Klein 1974; Faith 2012; supplementary fig. S9 and table S18, Supplementary Material online). It is derived from stratum RB, which is associated with accelerator mass spectroscopy radiocarbon dates of $8,447 \pm 39$ ¹⁴C years BP (9,545–9,460 cal years BP) and $8,550 \pm 39$ ¹⁴C years BP (9,520–9,305 cal years BP; Loftus et al. 2016). A Bayesian age model for the stratigraphic sequence at Nelson Bay Cave suggests the material derived from stratum RB broadly dates to between 9,800 and 9,300 cal years BP (Loftus et al. 2016). The associated artifacts belong to the Later Stone Age Oakhurst industry, which is a flake-based technology with few microliths or formal lithic tools (Deacon 1984). In contrast to the Pleistocene levels at Nelson Bay Cave, blue antelope are relatively uncommon in RB, with the dominant ungulates including Cape grysbok (*Raphicerus melanotis*), bushbuck (*Tragelaphus scriptus*), and bushpig (*Potamochoerus larvatus*) (Klein 1972, 1983), all of which presumably favour more closed habitats than expected for blue antelope.

Laboratory Procedures

DNA Preparation

We extracted DNA from all fossil samples following Dabney et al. (2013), using columns of Roche's High Pure Viral Nucleic Acid Kit for purification. Subsequently, we built single-stranded libraries from these extracts according to Gansauge et al. (2017), employing an additional initial 15 min incubation step with 0.5 µl USER Enzyme for Uracil removal (modified from Meyer et al. 2012). We used a maximum of 13 ng DNA as input for library construction. To determine the optimal number of amplification cycles for the subsequent dual-indexing PCR, we performed a qPCR (Thermo Scientific PikoReal Real-Time PCR System). Extraction and library blanks were run

alongside all samples to check for the presence of contamination. All pre-PCR lab work was conducted in dedicated aDNA facilities at the University of Potsdam, Germany. The single-stranded library of the historical sample NRM 590107 was prepared in the same way as described above (Hempel, Bibi, et al. 2021). All libraries from fossil specimens were test sequenced on an Illumina NextSeq500 using custom primers (Gansauge and Meyer 2013; Paijmans et al. 2017) at the University of Potsdam to determine their endogenous DNA content. Only one sample from Nelson Bay Cave (NBC RB4 D3, dP₄, fig. 1C) yielded sufficient endogenous DNA content for deeper sequencing. Therefore, we sequenced the library of NBC RB4 D3 using custom primers in one run on an Illumina NextSeq500 at the University of Potsdam, generating 75 bp single-end reads, and in another run on a NovaSeq6000 at the SciLifeLab, Sweden, generating 100 bp paired-end reads. We further sequenced the library of NRM 590107 using custom primers in three runs on an Illumina NextSeq500 at the University of Potsdam, generating 75 bp single-end reads, and on one run on a NovaSeq6000 at the SciLifeLab, generating 100 bp paired-end reads. In addition, for NRM 590107, we used 75 bp single-end read data generated from one run in Hempel, Bibi, et al. (2021) (SRR20324702, supplementary table S2, Supplementary Material online).

Bioinformatic Procedures and Analyses

Nuclear Genome

Data Preprocessing and Read Mapping

We processed single- and paired-end reads separately prior to duplicate removal but combined all single-end runs of NRM 590107 before processing. We used Cutadapt v2.8 (Martin 2011) to trim Illumina adapter sequences (1 bp overlap) and to remove reads shorter than 30 bp. We merged paired-end reads with FLASH v1.2.11 (Magoč and Salzberg 2011) using a maximum overlap of 100 bp and discarded all unmerged reads. Subsequently, we mapped the resulting reads to the nuclear genome of the scimitar-horned oryx (*Oryx dammah*; https://www.dnazon.org/assemblies/Oryx_dammah; Humble et al. 2020) using the BWA aln algorithm v0.7.17 (Li and Durbin 2009) and default settings. For quality filtering, we used SAMtools view v1.10 (Li et al. 2009) to remove reads with a mapping quality of <30, discarding unmapped reads, and then sorted bam files with SAMtools sort. We then merged all reads from a single individual with SAMtools merge and performed duplicate removal with Picard MarkDuplicates v2.22.4 (Picard Toolkit 2020 — <http://broadinstitute.github.io/picard>). We ran mapDamage v2.2.0 (Jónsson et al. 2013) and rescaled the bam file using the rescale option (—rescale) to decrease the quality of misincorporations that are likely caused by aDNA damage.

We used published raw sequencing read data of three roan antelopes (*H. equinus*; Gonçalves et al. 2021), eight sable antelopes (*H. niger*; Koepfli et al. 2019), and the

scimitar-horned oryx (*O. dammah*; [Humble et al. 2020](#); [supplementary table S4, Supplementary Material online](#)), all from contemporary samples, in our analyses. The reads for these samples were treated in the same way as described above with the exception that merged and unmerged reads were both mapped, that the maximum overlap parameter in FLASH was adjusted according to sequencing cycle length and that no rescaling was performed. For one roan antelope sample (10954) and the scimitar-horned oryx sample (SB20612), both from 10X Genomics libraries, 22 bp were trimmed from R1 after adapter trimming with Cutadapt using FASTA/Q Trimmer from the FASTX-Toolkit v0.0.14 (http://hannonlab.cshl.edu/fastx_toolkit).

As sex chromosomes and mitochondrial genomes have different inheritance patterns relative to autosomes and could bias downstream analyses, we removed 53 scaffolds that were identified to likely represent X and Y chromosomes and the mitochondrial genome in the scimitar-horned oryx reference genome ([Humble et al. 2020](#); [Hempel, Westbury, et al. 2021](#)).

As input fasta files for *D* statistics ([Green et al. 2010](#); [Durand et al. 2011](#)), the nuclear diversity estimates and Bayesian molecular dating, we generated pseudohaploid consensus sequences for all specimens using Consensify ([Barlow et al. 2020](#)). We generated the base count input file using ANGSD v0.923 ([Korneliussen et al. 2014](#); -minQ 30, -minMapQ 30, -uniqueonly 1, -remove_bads 1, -baq 2, -dumpCounts 3, -C 0, -only_proper_pairs 0, -doCounts 1, -trim 0). For the fossil and historical blue antelope specimens, the rescaled bam files from mapDamage were used as input files. We ran Consensify with twice the mean coverage of each sample as the maxDepth parameter and using only autosomal scaffolds >1 Mb. To check if sequence coverage had an effect on downstream results, we generated an additional set of subsampled files for all individuals (fossil, historical and contemporary) with SAMtools view, setting the baseline to the sample with the lowest mean coverage (2.14X, NBC RB4 D3) before running Consensify.

For the sliding window tree analyses, we generated pseudohaploid consensus sequences using random read sampling (-doFasta 1) in ANGSD and the following parameter settings: -minQ 30, -minMapQ 30, -uniqueonly 1, -only_proper_pairs 0, -remove_bads 1, -baq 2, -C 0, -explode 1, -doCounts 1, -trim 0, -basesPerLine 70. We only included autosomal scaffolds >1 Mb ([supplementary table S6, Supplementary Material online](#)). For the fossil and historical specimens of blue antelope, the rescaled bam files from mapDamage were used as input files.

Principal Component Analysis

We performed a principal component analysis in ANGSD by generating a covariance matrix (-doCov 1) applying a consensus base call approach (-doIBS 2), removing singletons (-minMinor 2) and transitions (-rmTrans 1), using only positions where all individuals had coverage (-minInd 13), and the following parameters: -doCounts 1, -makeMatrix 1,

-minQ 30, -minMapQ 30, -minInddepth 2, -uniqueonly 1, -only_proper_pairs 0, -remove_bads 1, -baq 2, -trim 0, -C 0, -doMajorMinor 1, -GL 2. We included all roan, all sable and all blue antelope individuals in this analysis.

Species Tree Inference

We constructed a neighbor joining tree using the nuclear genome data from the two blue, three roan ([Gonçalves et al. 2021](#)) and eight sable antelopes ([Koepfli et al. 2019](#)), along with the scimitar-horned oryx (SB20612, [Humble et al. 2020](#)) as outgroup to examine the dominant phylogenetic signal. The rescaled bam files from mapDamage for the fossil and historical blue antelope specimens as well as the bam files for all contemporary individuals were used as input files. We generated the input distance matrix in ANGSD using a consensus base call approach (-doIBS 2), removing singletons (-minMinor 2) and transitions (-rmTrans 1), and using only positions where all individuals had coverage (-minInd 14) (-doCounts 1, -makeMatrix 1, -minQ 30, -minMapQ 30, -minInddepth 2, -uniqueonly 1, -only_proper_pairs 0, -remove_bads 1, -baq 2, -trim 0, -C 0, -doMajorMinor 1, -GL 2). We used FastME v2.1.6.1 ([Lefort et al. 2015](#)) to generate a neighbor joining tree from the distance matrix using default parameters. The tree was visualized with FigTree v1.4.3 (<https://github.com/rambaut/figtree>).

To gain further confidence on our species tree estimate, we performed two other analyses. First, we inferred the species tree while accounting for incomplete lineage sorting and gene flow. We ran a sliding window tree analysis using the tool WindowTrees v1.0.0 (<https://github.com/achimklittich/WindowTrees>) with fasta files generated from random read sampling as input to generate non-overlapping sliding windows as input to infer phylogenies per window using IQ-TREE v2.2.0 ([Minh, Schmidt, et al. 2020](#)). We used binary mode to exclude transitions (—binary) and a missing data threshold of 50% (-N 0.5) with a window size of 20 kb (-w 20000) and a gap size of 80 kb (-lw 80000) between windows. For this analysis, only one individual of each species was used (roan: 10954, sable: SB2152, blue antelope: NBC RB4 D3). The scimitar-horned oryx was used as outgroup (SB20612; —outgroup). We used the resulting phylogenies while adding the mitochondrial genomes (without control regions) as an additional window as input for ASTRAL v4.10 ([Rabiee et al. 2019](#)) to infer the species tree under the multispecies coalescent with local posterior probability branch supports. Second, we inferred the tree using a concatenation of these windows and maximum likelihood under a GTR + R6 model of substitution ([Kalyaanamoorthy et al. 2017](#)), implemented in IQ-TREE2, and bootstrap support with 1,000 replicates, as implemented using the UFboot2 approximation ([Hoang et al. 2018](#)). Traditional phylogenetic branch supports tend to have maximal values, so gene- and site-concordance factor branch supports were also inferred using IQ-TREE2 ([Minh, Hahn, et al. 2020](#)) to produce a more nuanced picture of branch support. All phylogenetic

methods led to identical inferences of the species tree topology.

Fossil-Calibrated Phylogeny

We fossil-calibrated the species phylogeny generated from the combined nuclear and mitochondrial data set. To avoid the impact of incomplete lineage sorting on molecular dating (Mendes and Hahn 2016), windows were filtered to include only those that had a concordant phylogenetic signal with the species tree, as inferred from the ASTRAL and neighbor joining analyses (see above). Similarly, we avoided further phylogenetic biases by using trees with strong branch supports (bootstrap support >90) and low rate variation among lineages (CoV in root-to-tip length <0.1; Vankan et al. 2022). We used the following individuals: the early Holocene blue antelope (NBC RB4 D3), one roan antelope (10954, Gonçalves et al. 2021), one sable antelope (SB2152, Koepfli et al. 2019) and the scimitar-horned oryx (SB20612, Humble et al. 2020) as outgroup. As input files, we used the fasta files generated with Consensify (see above) but including only transversions. For calibration, we used a uniform prior between 3.6 and 4.5 Ma for the split between Oryx and *Hippotragus* (Vrba and Gatesy 1994; Deino 2011; Gentry 2011; for further explanations see Bibi 2013), with a soft maximum bound. A birth-death process was used as tree prior, and rates across lineages were assumed to follow an uncorrelated gamma-distributed clock model. We used approximate likelihood computation as implemented in MCMCTree (in PAML v4.9; dos Reis and Yang 2011) with an MCMC chain of 10M steps, discarding the first million as burn-in. We verified that the analysis reached convergence by verifying all parameter traces and replicating the analysis to confirm convergence to an identical optimum (supplementary files S3–S10, Supplementary Material online). The tree was visualized with FigTree.

D statistics

For D statistics analysis, we used the fasta files generated with Consensify of the roan and sable antelope individuals with the highest coverage (10954, Gonçalves et al. 2021, and SB2152, Koepfli et al. 2019) together with the scimitar-horned oryx as outgroup (SB20612, Humble et al. 2020) and either the fossil or the historical blue antelope specimen. We used the topology resulting from the 20 kb sliding window multispecies coalescent and neighbor joining analyses (see above, fig. 2 and supplementary fig. S3, Supplementary Material online), placing the sable antelope in position 1, the blue antelope in position 2, and the roan antelope in position 3 (fig. 3B). We conducted D statistics/abbababa test with the tool Dstat (transversion only version, <https://github.com/jacahill/Admixture>) and calculated the standard error using the weighted_block_jackknife_D tool with a 1-Mb window size. Positive D values indicate an excess of derived alleles for individuals in positions 2 and 3 (ABBA sites), whereas negative D values indicate an excess of derived alleles for individuals in positions 1 and 3 (BABA sites). From this,

we calculated Z-scores with a Z-score $>|3|$ defined as significant.

Inferences of Gene Flow Directionality and Timing

To investigate the direction and timing of gene flow, we used a sliding window tree approach. As input, we used the randomly sampled fasta files (see above). We then used the tool WindowTrees (<https://github.com/achimklittich/WindowTrees>) to generate non-overlapping sliding window maximum-likelihood phylogenies using RAxML v8.2.12 (Stamatakis 2014) in binary mode to exclude transitions (—binary), a window size of 100 kb (-w 100000) and a threshold for missing data of 50% (-N 0.5). Prior to the introduction of the WindowTrees tool, this procedure was already successfully used to determine gene flow direction in other studies (Barlow et al. 2018; Westbury et al. 2020; Pajjmans et al. 2021). This was performed for all possible combinations with two roan, one sable, and one blue antelope using the following individuals — roan: 10954, He108; sable: SB2152, HN216; blue antelope: NBC RB4 D3, NRM 590107. The scimitar-horned oryx (SB20612) was defined as outgroup in each case (—outgroup).

In addition, we used the resulting phylogenies from the sliding window tree analysis that used WindowTrees in binary mode with a missing data threshold of 50% (-N 0.5), a window size of 20 kb (-w 20000) and a gap size of 80 kb (-lw 80000) between windows (see above). We examined the hypothesis of gene flow in the direction of blue into roan antelope using estimates of gene trees and their phylogenetic branch lengths. Under a scenario of gene flow from blue into roan antelope, the portion of introgressed loci will show a signal of more recent common ancestry between the roan and the sable antelope relative to the species tree topology. On the other hand, a scenario of gene flow in the direction from roan into blue antelope will lead all of the loci to have a signal of similar times of common ancestry between roan and sable antelope in accordance with the species tree topology (fig. 4A). To examine these hypotheses, we extracted the sum of phylogenetic branch lengths separating roan and sable antelope instead of roan and blue antelope as to avoid biases that may influence the branch length, for example, possible DNA damage and higher sequencing errors, due to lower coverage, as expected from the fossil specimen. We then compared this signal between the gene trees in which roan and blue antelope are sister species (potentially including introgressed regions) against gene trees in which sable and blue antelope are sister species (showing distances between common ancestors of those species). To exclude extremely high and extremely low distances, which likely arise due to the high variance in estimates of branch lengths with negligible information available, we filtered out distances of <0.0002 and >0.9 . For any occurrence of gene flow from the blue into the roan antelope, a bimodal distribution would have been expected due to the relatively shorter interspecific branch lengths that would arise. Genetic distances from gene trees were extracted using the R package ape v5.5 (Paradis and

[Schliep 2019; supplementary file S11, Supplementary Material online](#)).

Species-wide Nuclear Diversity Comparisons

We performed within species pairwise comparisons to estimate the species-wide nuclear diversity for each species within the genus *Hippotragus*. We implemented an approach that we show can be used for low coverage data and take the patterns of unusual DNA damage found in blue antelope specimen NRM 590107 into account.

We used the fasta files generated with Consensify from the two blue, three roan, and eight sable antelope samples, and the single outgroup scimitar-horned oryx, and filtered those by excluding positions with missing data and positions where all individuals had the same allele (uninformative sites) using a custom perl script. We then performed pairwise difference estimates for the individuals of each species by counting the number of different alleles while excluding all potential aDNA damage (transitions) and all differences resembling the damage pattern found in NRM 590107 (guanine to thymine and cytosine to adenine and vice versa).

The values were normalized by dividing them by the total number of positions after filtering. We plotted the values for each pairwise comparison together with the mean for roan and sable antelope. We additionally ran the analysis with the input files that were subsampled to 2.14 \times mean coverage before running Consensify to test for the effects of sequence coverage.

To examine how the number of differences between individuals compares to a more standard measure of diversity, that is, heterozygosity, we calculated allele frequencies using genotype likelihoods for each roan and sable antelope individual using ANGSD, setting the -setMaxDepth parameter to twice the mean coverage and with the following parameter settings: -setMinDepthInd 5, -minInd 1, -doCounts 1, -GL 2, -doSaf 1, -fold 1, -minQ 30, -minMapQ 30, -uniqueonly 1, -remove_bads 1, -only_proper_pairs 0, -trim 0, -C 0, -baq 2. Next, we calculated the site frequency spectrum using realSFS in ANGSD. This analysis was performed once using the full data set and once with the bam files subsampled with SAMtools view to the lowest mean coverage of a specimen in the roan/sable antelope data set (4.26 \times of sable antelope SB1954) to ensure no bias could result from uneven coverage. We plotted the values for the subsampled calculations per individual together with the mean for each species.

Mitochondrial Genome

Read Mapping

We treated the reads for the mitochondrial genome of NBC RB4 D3 in the same way as described for the nuclear genome but used the mitochondrial genome of the blue antelope (MW222233, [Hempel, Bibi, et al. 2021](#)) as reference and removed duplicates with MarkDupsByStartEnd (<https://github.com/dariober/Java-cafe/tree/master/MarkDupsByStartEnd>). We generated a consensus sequence in Geneious R10 v10.2.3 ([Kearse et al. 2012](#), <https://www.geneious.com>) using an 85% majority rule threshold for base calling, a minimum coverage of 3X and the “trim to reference” option. To improve the

coverage at the end of the sequence, we mapped and filtered the data again as described above, but used a reference with 200 bp shifted from the end to the start of the reference, considering the circular nature of the mitochondrial genome. We called a consensus sequence as described before and subsequently moved the 200 bp back to the end of the sequence. Then we called a consensus sequence from both sequences using a 50% majority rule threshold for base calling (option “50% — Strict: Bases matching at least 50% of the sequences”).

We generated mitochondrial genomes from the raw sequencing data of all roan and sable antelope specimens and the outgroup scimitar-horned oryx specimen for which assembled mitogenomes were not available (roan: He95, He108, 10954; sable antelope: HN216, HN250; scimitar-horned oryx: SB20612; [supplementary table S5, Supplementary Material online](#)). We treated the data in the same way as described for the nuclear genomes while using conspecific mitochondrial genomes as references (roan and sable antelope and scimitar-horned oryx: JN632647, JN632648, JN632677; [Hassanin et al. 2012](#)) and employing a second mapping step as described for NBC RB4 D3 but varying the length of the reference part that was moved for the second mapping (see above) to be twice the sequencing cycle length of each sample.

Maximum-likelihood Phylogenies From Mitochondrial Genomes

We built an alignment with the consensus sequences of the two blue, three roan, and eight sable antelopes using the MAFFT algorithm v7.450 ([Katoh et al. 2002](#); [Katoh and Standley 2013](#)) and default parameters as implemented in Geneious. We used the scimitar-horned oryx as outgroup (SB20612). We removed the control region from all sequences prior to aligning them due to their limited alignability for different species ([supplementary files S12 and S13, Supplementary Material online](#)). We generated two maximum-likelihood phylogenies with 1,000 bootstrap replicates each using RAxML v8.2.12, once with the GTR + G substitution model and the other with the BINGAMMA model ([Stamatakis 2014](#)). Bootstrap branch support was calculated using 1,000 replicates and the UFboot2 implementation, as done with the nuclear data. For the latter, the alignment was first transformed into binary format to only score transversions. The tree was visualized with FigTree.

Fossil-Calibrated Phylogeny

We generated a fossil-calibrated phylogeny using the same alignment as for the maximum-likelihood phylogeny but extracted the following individuals to ensure comparability with our nuclear phylogeny: the early Holocene blue antelope (NBC RB4 D3), the roan antelope (10954, [Gonçalves et al. 2021](#)), the sable antelope (SB2152, [Koepfli et al. 2019](#)) and the scimitar-horned oryx (SB20612, [Humble et al. 2020](#)) as outgroup. For this analysis we used the same tree topology, fossil calibration, Bayesian implementation, analysis parameters and diagnostics as used for the nuclear data set. The tree was visualized with FigTree.

Haplotype Network with Mitochondrial Genomes

To determine the extent of differences between our fossil and the previously published historical specimens of the blue antelope, we aligned the mitochondrial genome of NBC RB4 D3 to the other two available complete mitochondrial blue antelope genomes (MW222233, MW222234, [Hempel, Bibi, et al. 2021, supplementary table S17, Supplementary Material online](#)) using the MAFFT algorithm with default settings as implemented in Geneious. We removed all ambiguities/missing data ([supplementary files S14 and S15, Supplementary Material online](#)). Subsequently, we constructed a median-joining network with POPART v1.7 ([Bandelt et al. 1999; Leigh and Bryant 2015](#)) and calculated the number of segregating sites and nucleotide diversity. In addition, we aligned the mitochondrial genome of NBC RB4 D3 with the two available complete and the two partial mitochondrial genomes of the blue antelope (MW228401, MW228402, [Hempel, Bibi, et al. 2021, supplementary table S17, Supplementary Material online](#)) using again the MAFFT algorithm with default settings as implemented in Geneious and repeated all steps described for the alignment with the complete mitochondrial genomes to generate a median-joining network and determine the number of segregating sites and the nucleotide diversity using POPART.

Supplementary Material

[Supplementary data](#) are available at *Molecular Biology and Evolution* online including alignments for the haplotype networks and maximum-likelihood phylogenies and the R scripts for the sliding window tree genetic distance analysis and the phylogenomic analysis.

Acknowledgments

This work was supported by the Deutsche Forschungsgemeinschaft (DFG, German Research Foundation; project numbers 315696891, HO 3492/3-1, BI 1879/2-1 to M.H. and F.B.) and by the Swedish Research Council (2017-04647) and FORMAS (2018-01640 both to L.D.). The authors acknowledge the support of Iziko Museums of South Africa, Heritage Western Cape, Cape Nature, Eastern Cape Provincial Heritage Resources Authority, and South African Heritage Resources Agency. They thank Wendy Black, Wilhelmina Seonna, and Mark De Benedictis for access to and support while at the Archaeology Unit, Iziko Museums of South Africa. They thank Margarida Gonçalves and Raquel Godinho for providing the raw data for the roan antelope sample 10954 and Gaik Tamazian and Pavel Dobrynin for providing the raw data for the sable antelope samples HN216 and HN250. The authors thank Stefanie Hartmann for providing the custom perl script for data filtering and Michaela Preick for laboratory work in screening samples. The authors also

acknowledge support from Science for Life Laboratory, the Knut and Alice Wallenberg Foundation, the National Genomics Infrastructure funded by the Swedish Research Council, and Uppsala Multidisciplinary Center for Advanced Computational Science for assistance with massively parallel sequencing and access to the UPPMAX computational infrastructure.

Author Contributions

The study was designed by E.H., F.B., J.T.F., J.S.B., M.H., and M.V.W. Funding was acquired by F.B. and M.H. J.T.F. identified and measured specimens. E.H. sampled the specimens and performed laboratory work. E.H., D.A.D. and M.V.W. performed DNA analyses with input from M.H. A.M.K. wrote the WindowTrees program. E.H. and M.V.W. wrote the manuscript with input from F.B., J.T.F., K.-P.K., D.A.D., D.C.K., and M.H. Resources were supplied by L.D. and M.H. Final editing and manuscript preparation was coordinated by E.H. All contributing authors read and agreed to the final manuscript.

Data Availability

The BioProject number of this project in GenBank is PRJNA776140. The complete mitochondrial genome of the fossil blue antelope specimen NBC RB4 D3 is available at GenBank under the accession number ON101842. The untrimmed raw data were uploaded for the fossil specimen NBC RB4 D3 to the Sequence Read Archive under SRR19087237, SRR19086850, SRR19086815, SRR18968074, and SRR18912172 and for the historical specimen NRM 590107 under SRR18936629–SRR18936631 and SRR18753915. For NRM 590107 run SRR20324702 from BioProject, PRJNA776136 was used as well.

References

- Avery DM. 2019. *A fossil history of southern African land mammals*. Cambridge, New York, Port Melbourne, New Delhi: Cambridge University Press.
- Bandelt HJ, Forster P, Röhl A. 1999. Median-joining networks for inferring intraspecific phylogenies. *Mol Biol Evol*. **16**:37–48.
- Barlow A, Cahill JA, Hartmann S, Theunert C, Xenikoudakis G, Fortes GG, Pajjmans JLA, Rabeder G, Frischauft C, Grandal-d'Anglade A, et al. 2018. Partial genomic survival of cave bears in living brown bears. *Nat Ecol Evol*. **2**:1563–1570.
- Barlow A, Hartmann S, Gonzalez J, Hofreiter M, Pajjmans JLA. 2020. Consensify: a method for generating pseudohaploid genome sequences from palaeogenomic datasets with reduced error rates. *Genes (Basel)*. **11**:50.
- Barlow A, Pajjmans JLA, Alberti F, Gasparyan B, Bar-Oz G, Pinhasi R, Foronova I, Puzachenko AY, Pacher M, Dalén L, et al. 2021. Middle Pleistocene genome calibrates a revised evolutionary history of extinct cave bears. *Curr Biol*. **31**:1771–1779.e7.
- Bibi F. 2013. A multi-calibrated mitochondrial phylogeny of extant Bovidae (Artiodactyla, Ruminantia) and the importance of the fossil record to systematics. *BMC Evol Biol*. **13**:166.
- Bollongino R, Tresset A, Vigne J-D. 2008. Environment and excavation: pre-lab impacts on ancient DNA analyses. *C R Palevol*. **7**: 91–98.

- Brink JS, Lee-Thorp JA. 1992. The feeding niche of an extinct springbok, *Antidorcas bondi* (Antelopini, Bovidae), and its paleoenvironmental meaning. *S Afr J Sci.* **88**:227–229.
- Cawthra HC, Compton JS, Fisher EC, MacHutchon MR, Marean CW. 2015. Submerged shorelines and landscape features offshore of Mossel Bay, South Africa. *Geol Soc Spec Publ.* **411**:219–233.
- Cawthra HC, Cowling RM, Andò S, Marean CW. 2020. Geological and soil maps of the Palaeo-Agulhas plain for the last glacial maximum. *Quat Sci Rev.* **235**:105858.
- Ceballos G, Ehrlich PR, Barnosky AD, García A, Pringle RM, Palmer TM. 2015. Accelerated modern human-induced species losses: entering the sixth mass extinction. *Sci Adv.* **1**:e1400253.
- Compton JS. 2011. Pleistocene sea-level fluctuations and human evolution on the southern coastal plain of South Africa. *Quat Sci Rev.* **30**:506–527.
- Copeland SR, Cawthra HC, Fisher EC, Lee-Thorp JA, Cowling RM, le Roux PJ, Hodgkins J, Marean CW. 2016. Strontium isotope investigation of ungulate movement patterns on the Pleistocene Paleo-Agulhas Plain of the Greater Cape Floristic Region, South Africa. *Quat Sci Rev.* **141**:65–84.
- Couto AN, Taurozzi AJ, Mackie M, Jensen TZT, Collins MJ, Sealy J. 2021. Palaeoproteomics confirm earliest domesticated sheep in southern Africa ca. 2000 BP. *Sci Rep.* **11**:6631.
- Crossman CA, Taylor EB, Barrett-Lennard LG. 2016. Hybridization in the Cetacea: widespread occurrence and associated morphological, behavioral, and ecological factors. *Ecol Evol.* **6**:1293–1303.
- Dabney J, Knapp M, Glocke I, Gansauge M-T, Weihmann A, Nickel B, Valdiosera C, García N, Pääbo S, Arsuaga J-L, et al. 2013. Complete mitochondrial genome sequence of a middle Pleistocene cave bear reconstructed from ultrashort DNA fragments. *Proc Natl Acad Sci U S A.* **110**:15758–15763.
- Deacon J. 1984. *The Later Stone Age of southernmost Africa*. Oxford: BAR.
- Deacon HJ, Thackeray JF. 1984. Late Pleistocene environmental changes and implications for the archaeological record in southern Africa. In: Vogel JC, editor. *Late Cainozoic palaeoclimates of the Southern Hemisphere*. Rotterdam: Balkema. p. 375–390.
- Deino AL. 2011. 40Ar/39Ar dating of Laetoli, Tanzania. In: Harrison T, editor. *Paleontology and geology of Laetoli: human evolution in context*. Vol. 1. New York: Springer. p. 77–97.
- DeWoody JA, Harder AM, Mathur S, Willoughby JR. 2021. The long-standing significance of genetic diversity in conservation. *Mol Ecol.* **30**:4147–4154.
- d'Huart J-P, Grubb P. 2001. Distribution of the common warthog (*Phacochoerus africanus*) and the desert warthog (*Phacochoerus aethiopicus*) in the Horn of Africa. *Afr J Ecol.* **39**: 156–169.
- Dingle RV, Rogers J. 1972. Pleistocene palaeogeography of the Agulhas Bank. *Trans R Soc S Afr.* **40**:155–165.
- dos Reis M, Yang Z. 2011. Approximate likelihood calculation on a phylogeny for Bayesian estimation of divergence times. *Mol Biol Evol.* **28**:2161–2172.
- du Plessis SF. 1969. The past and present geographical distribution of the Perissodactyla and Artiodactyla in southern Africa.
- Durand EY, Patterson N, Reich D, Slatkin M. 2011. Testing for ancient admixture between closely related populations. *Mol Biol Evol.* **28**: 2239–2252.
- Dussex N, van der Valk T, Morales HE, Wheat CW, Díez-del-Molino D, von Seth J, Foster Y, Kutschera VE, Guschanski K, Rhie A, et al. 2021. Population genomics of the critically endangered kākāpō. *Cell Genomics.* **1**:100002.
- Edwards CJ, Suchard MA, Lemey P, Welch JJ, Barnes I, Fulton TL, Barnett R, O'Connell TC, Coxon P, Monaghan N, et al. 2011. Ancient hybridization and an Irish origin for the modern polar bear matriline. *Curr Biol.* **21**:1251–1258.
- Faith JT. 2011. Late Quaternary megafaunal extinctions in southern Africa's Cape Floral Region.
- Faith JT. 2012. Conservation implications of fossil roan antelope (*Hippotragus equinus*) in Southern Africa's Cape floristic region. In: Louys J, editor. *Paleontology in ecology and conservation*. Berlin, Heidelberg: Springer. p. 239–251.
- Faith JT. 2013. Taphonomic and paleoecological change in the large mammal sequence from Boomplaas Cave, Western Cape, South Africa. *J Hum Evol.* **65**:715–730.
- Faith JT. 2014. Late Pleistocene and Holocene mammal extinctions on continental Africa. *Earth-Sci Rev.* **128**:105–121.
- Faith JT, Behrensmeier AK. 2013. Climate change and faunal turnover: testing the mechanics of the turnover-pulse hypothesis with South African fossil data. *Paleobiology* **39**:609–627.
- Faith JT, Thompson JC. 2013. Fossil evidence for seasonal calving and migration of extinct blue antelope (*Hippotragus leucophaeus*) in southern Africa. *J Biogeogr.* **40**:2108–2118.
- Fisher EC, Bar-Matthews M, Jerardino A, Marean CW. 2010. Middle and late Pleistocene paleoscape modeling along the southern coast of South Africa. *Quat Sci Rev.* **29**:1382–1398.
- FitzSimons FW. 1920. The bluebuck or blaauwbok (*Hippotragus leucophaeus*). In: *The natural history of South Africa*. Vol. 3. London: Longmans, Green and Co. p. 97–105.
- Gansauge M-T, Gerber T, Glocke I, Korlević P, Lippik L, Nagel S, Riehl LM, Schmidt A, Meyer M. 2017. Single-stranded DNA library preparation from highly degraded DNA using T4 DNA ligase. *Nucleic Acids Res.* **45**:e79.
- Gansauge M-T, Meyer M. 2013. Single-stranded DNA library preparation for the sequencing of ancient or damaged DNA. *Nat Protoc.* **8**:737–748.
- Gentry AW. 2011. Bovidae. In: Harrison T, editor. *Paleontology and geology of Laetoli: human evolution in context*. Vol. 2. Dordrecht, Heidelberg, London, New York: Springer. p. 363–465.
- Gonçalves M, Siegmund HR, van Vuuren BJ, Koepfli K-P, Ferrand N, Godinho R. 2021. *De novo* whole-genome assembly and resequencing resources for the roan (*Hippotragus equinus*), an iconic African antelope. *G3* **11**:jkab002.
- Green RE, Krause J, Briggs AW, Maricic T, Stenzel U, Kircher M, Patterson N, Li H, Zhai W, Fritz MHY, et al. 2010. A draft sequence of the neandertal genome. *Science* **328**:710–722.
- Hack MA, East R, Rubenstein DL. 2008. *Equus quagga* ssp. *quagga*. The IUCN red list of threatened species:e.T7957A12876306.
- Hailer F, Kutschera VE, Hallström BM, Klässert D, Fain SR, Leonard JA, Arnason U, Janke A. 2012. Nuclear genomic sequences reveal that polar bears are an old and distinct bear lineage. *Science.* **336**:344–347.
- Harper F. 1945. Blaauwbok; blue-buck. In: *Extinct and vanishing mammals of the old world*. Baltimore: The Lord Baltimore Press. p. 698–700. <https://www.biodiversitylibrary.org/bibliography/19520>.
- Hassanin A, Delsuc F, Ropiquet A, Hammer C, Jansen van Vuuren B, Matthee C, Ruiz-Garcia M, Catzeffis F, Areskoug V, Nguyen TT, et al. 2012. Pattern and timing of diversification of Cetartiodactyla (Mammalia, Laurasiatheria), as revealed by a comprehensive analysis of mitochondrial genomes. *C R Biol.* **335**:32–50.
- Hempel E, Bibi F, Faith JT, Brink JS, Kalthoff DC, Kamminga P, Pajtmans JLA, Westbury MV, Hofreiter M, Zachos FE. 2021. Identifying the true number of specimens of the extinct blue antelope (*Hippotragus leucophaeus*). *Sci Rep.* **11**:2100.
- Hempel E, Westbury MV, Grau JH, Trinks A, Pajtmans JLA, Kliver S, Barlow A, Mayer F, Müller J, Chen L, et al. 2021. Diversity and paleodemography of the Addax (*Addax nasomaculatus*), a Saharan antelope on the verge of extinction. *Genes (Basel).* **12**:1236.
- Hoang DT, Chernomor O, von Haeseler A, Minh BQ, Vinh LS. 2018. UFBoot2: improving the ultrafast bootstrap approximation. *Mol Biol Evol.* **35**:518–522.
- Hofreiter M, Pajtmans JLA, Goodchild H, Speller CF, Barlow A, Fortes GG, Thomas JA, Ludwig A, Collins MJ. 2015. The future of ancient DNA: technical advances and conceptual shifts: prospects & overviews. *BioEssays* **37**:284–293.
- Hubbs CL. 1955. Hybridization between fish species in nature. *Syst Zool.* **4**:1–20.

- Humble E, Dobrynin P, Senn H, Chuvan J, Scott AF, Mohr DW, Dudchenko O, Omer AD, Colaric Z, Aiden EL, et al. 2020. Chromosomal-level genome assembly of the scimitar-horned oryx: insights into diversity and demography of a species extinct in the wild. *Mol Ecol Resour.* **20**:1668–1681.
- IUCN SSC Antelope Specialist Group. 2017. *Alcelaphus buselaphus* ssp. *buselaphus*. The IUCN Red List of Threatened Species 2017:e.T813A50181474.
- Jansson G, Thulin C-G, Pehrson Å. 2007. Factors related to the occurrence of hybrids between brown hares *Lepus europaeus* and mountain hares *L. timidus* in Sweden. *Ecography* **30**:709–715.
- Jónsson H, Ginolhac A, Schubert M, Johnson PLF, Orlando L. 2013. MapDamage2.0: fast approximate Bayesian estimates of ancient DNA damage parameters. *Bioinformatics* **29**:1682–1684.
- Kalyaanamoorthy S, Minh BQ, Wong TKF, von Haeseler A, Jermiin LS. 2017. ModelFinder: fast model selection for accurate phylogenetic estimates. *Nat Methods.* **14**:587–589.
- Kardos M, Armstrong EE, Fitzpatrick SW, Hauser S, Hedrick PW, Miller JM, Tallmon DA, Funk WC. 2021. The crucial role of genome-wide genetic variation in conservation. *Proc Natl Acad Sci U S A.* **118**:e2104642118.
- Katoh K, Misawa K, Kuma K, Miyata T. 2002. MAFFT: a novel method for rapid multiple sequence alignment based on fast Fourier transform. *Nucleic Acids Res.* **30**:3059–3066.
- Katoh K, Standley DM. 2013. MAFFT Multiple sequence alignment software version 7: improvements in performance and usability. *Mol Biol Evol.* **30**:772–780.
- Kearse M, Moir R, Wilson A, Stones-Havas S, Cheung M, Sturrock S, Buxton S, Cooper A, Markowitz S, Duran C, et al. 2012. Geneious basic: an integrated and extendable desktop software platform for the organization and analysis of sequence data. *Bioinformatics* **28**:1647–1649.
- Kerley GIH, Pressey RL, Cowling RM, Boshoff AF, Sims-Castley R. 2003. Options for the conservation of large and medium-sized mammals in the Cape Floristic Region hotspot, South Africa. *Biol Conserv.* **112**:169–190.
- Kerley GIH, Sims-Castley R, Boshoff AF, Cowling RM. 2009. Extinction of the blue antelope *Hippotragus leucophaeus*: modeling predicts non-viable global population size as the primary driver. *Biodivers Conserv.* **18**:3235–3242.
- Klein RG. 1972. The late Quaternary mammalian fauna of Nelson Bay Cave (Cape Province, South Africa): its implications for megafaunal extinctions and environmental and cultural change. *Quat Res.* **2**:135–142.
- Klein RG. 1974. On the taxonomic status, distribution and ecology of the blue antelope, *Hippotragus leucophaeus* (Pallas, 1766). *Ann S Afr Mus.* **65**:99–143.
- Klein RG. 1976. The mammalian fauna of the Klasies River Mouth Sites, Southern Cape Province, South Africa. *S Afr Archaeol Bull.* **31**:75.
- Klein RG. 1980. Environmental and ecological implications of large mammals from upper Pleistocene and Holocene sites in southern Africa. *Ann S Afr Mus.* **81**:223–283.
- Klein RG. 1983. Palaeoenvironmental implications of Quaternary large mammals in the fynbos region. In: Deacon HJ, Hendrey QB, Lambrechts JNN, editors. *Fynbos paleoecology: a preliminary synthesis*. South African National Scientific Programmes Rep. Pretoria. Republic of South Africa: CSIR. p. 116–138.
- Klein RG. 1987. The extinct blue antelope. *Sagittarius* **2**:20–23.
- Klein RG, Avery G, Cruz-Uribe K, Steele TE. 2007. The mammalian fauna associated with an archaic hominin skullcap and later Acheulean artifacts at Elandsfontein, Western Cape Province, South Africa. *J Hum Evol.* **52**:164–186.
- Klein RG, Cruz-Uribe K. 2016. Large mammal and tortoise bones from Elands Bay Cave (South Africa): implications for Later Stone Age environment and ecology. *South Afr Humanit.* **29**:259–282.
- Koepfli K-P, Tamazian G, Wildt D, Dobrynin P, Kim C, Frandsen PB, Godinho R, Yurchenko AA, Komissarov A, Krasheninnikova K, et al. 2019. Whole genome sequencing and re-sequencing of the sable antelope (*Hippotragus niger*): a resource for monitoring diversity in ex situ and in situ populations. *G3.* **9**:1785–1793.
- Kohl FF. 1886. Ueber neue und seltene Antilopen des k. k. naturhistorischen Hofmuseums. *Ann K K Naturh Hofmus Wien.* **1**:75–86.
- Korneliussen TS, Albrechtsen A, Nielsen R. 2014. ANGSD: analysis of next generation sequencing data. *BMC Bioinform.* **15**:356.
- Kvam E, Tyrrell RM. 1997. Artificial background and induced levels of oxidative base damage in DNA from human cells. *Carcinogenesis* **18**:2281–2283.
- Larsen PA, Marchán-Rivadeneira MR, Baker RJ. 2010. Natural hybridization generates mammalian lineage with species characteristics. *Proc Natl Acad Sci U S A.* **107**:11447–11452.
- Lefort V, Desper R, Gascuel O. 2015. FastME 2.0: a comprehensive, accurate, and fast distance-based phylogeny inference program. *Mol Biol Evol.* **32**:2798–2800.
- Leigh JW, Bryant D. 2015. POPART: full-feature software for haplotype network construction. *Methods Ecol Evol.* **6**: 1110–1116.
- Li H, Durbin R. 2009. Fast and accurate short read alignment with Burrows-Wheeler transform. *Bioinformatics* **25**:1754–1760.
- Li H, Handsaker B, Wysoker A, Fennell T, Ruan J, Homer N, Marth G, Abecasis G, Durbin R, 1000 Genome Project Data Processing Subgroup. 2009. The sequence alignment/map format and SAMtools. *Bioinformatics* **25**:2078–2079.
- Lichtenstein H. 1811. *Reisen im südlichen Africa in den Jahren 1803, 1804, 1805 und 1806*. Berlin: C. Salfeld.
- Lichtenstein H. 1814. Die Gattung Antilope. *Ges Naturf Freunde Berlin Mag neuesten Entdeck gesammten Naturk* **6**:147–160, 163–182.
- Lipson M, Sawchuk EA, Thompson JC, Oppenheimer J, Tryon CA, Ranhorn KL, de Luna KM, Sirak KA, Olalde I, Ambrose SH, et al. 2022. Ancient DNA and deep population structure in sub-Saharan African foragers. *Nature* **603**:290–296.
- Liu S, Westbury MV, Dussex N, Mitchell KJ, Sinding M-HS, Heintzman PD, Duchêne DA, Kapp JD, von Seth J, Heiniger H, et al. 2021. Ancient and modern genomes unravel the evolutionary history of the rhinoceros family. *Cell* **184**:4874–4885.e16.
- Loftus E, Sealy J, Lee-Thorp J. 2016. New radiocarbon dates and Bayesian models for Nelson Bay Cave and Byneskranskop 1: implications for the South African Later Stone Age sequence. *Radiocarbon* **58**:365–381.
- Loubser J, Brink J, Laurens G. 1990. Paintings of the extinct blue antelope, *Hippotragus leucophaeus*, in the eastern Orange Free State. *S Afr Archaeol Bull.* **45**:106–111.
- Magoć T, Salzberg SL. 2011. FLASH: fast length adjustment of short reads to improve genome assemblies. *Bioinformatics* **27**: 2957–2963.
- Martin M. 2011. Cutadapt removes adapter sequences from high-throughput sequencing reads. *EMBnet.journal* **17**:10–12.
- Mathieson I, Abascal F, Vinner L, Skoglund P, Pomiña C, Mitchell P, Arthur C, Gurdasani D, Willerslev E, Sandhu MS, et al. 2020. An ancient baboon genome demonstrates long-term population continuity in southern Africa. *Genome Biol Evol.* **12**:407–412.
- Mendes FK, Hahn MW. 2016. Gene tree discordance causes apparent substitution rate variation. *Syst Biol.* **65**:711–721.
- Meyer M, Kircher M, Gansauge M-T, Li H, Racimo F, Mallick S, Schraiber J G, Jay F, Prüfer K, de Filippo C, et al. 2012. A high-coverage genome sequence from an archaic Denisovan individual. *Science* **338**:222–226.
- Minh BQ, Hahn MW, Lanfear R. 2020. New methods to calculate concordance factors for phylogenomic datasets. *Mol Biol Evol.* **37**:2727–2733.
- Minh BQ, Schmidt HA, Chernomor O, Schrempf D, Woodhams MD, von Haeseler A, Lanfear R. 2020. IQ-TREE 2: new models and efficient methods for phylogenetic inference in the genomic era. *Mol Biol Evol.* **37**:1530–1534.
- Mohr E. 1967. In: Herre W, Röhrs M, editors. *Der Blaubock Hippotragus leucophaeus (Pallas, 1766) — Eine Dokumentation*. Hamburg, Berlin: Paul Parey.

- Nohmi T, Kim S-R, Yamada M. 2005. Modulation of oxidative mutagenesis and carcinogenesis by polymorphic forms of human DNA repair enzymes. *Mutat Res.* **591**:60–73.
- Opperman H. 1987. *The Later Stone Age of the Drakensberg Range and its foothills*. Oxford: BAR.
- Paijmans JLA, Baleka S, Henneberger K, Taron UH, Trinks A, Westbury MV, Barlow A. 2017. Sequencing single-stranded libraries on the Illumina NextSeq 500 platform. Unpublished data. [cited 2020 Apr 12]. Available from: <http://arxiv.org/abs/1711.11004>.
- Paijmans JLA, Barlow A, Becker MS, Cahill JA, Fickel J, Förster DWG, Gries K, Hartmann S, Havmøller RW, Henneberger K, et al. 2021. African and Asian leopards are highly differentiated at the genomic level. *Curr Biol.* **31**:1872–1882.e5.
- Pallas PS. 1767. *Spicilegia zoologica quibus novae imprimis et obscurae animalium species*. Berlin: Gottlieb August Lange.
- Paradis E, Schliep K. 2019. Ape 5.0: an environment for modern phylogenetics and evolutionary analyses in R. *Bioinformatics* **35**: 526–528.
- Plug I. 1997. Late Pleistocene and Holocene hunter-gatherers in the eastern highlands of South Africa and Lesotho: a faunal interpretation. *J Archaeol Sci.* **24**:715–727.
- Rabiee M, Sayyari E, Mirarab S. 2019. Multi-allele species reconstruction using ASTRAL. *Mol Phylogenetics Evol.* **130**:186–296.
- Rakotoarivelo AR, O'Donoghue P, Bruford MW, Moodley Y. 2019. An ancient hybridization event reconciles mito-nuclear discordance among spiral-horned antelopes. *J Mammal.* **100**:1144–1155.
- Reich D, Green RE, Kircher M, Krause J, Patterson N, Durand EY, Viola B, Briggs AW, Stenzel U, Johnson PLF, et al. 2010. Genetic history of an archaic hominin group from Denisova Cave in Siberia. *Nature* **468**:1053–1060.
- Robinson TJ, Bastos AD, Halanych KM, Herzig B. 1996. Mitochondrial DNA sequence relationships of the extinct blue antelope *Hippotragus leucophaeus*. *Naturwissenschaften* **83**:178–182.
- Robinson TJ, Harley EH. 1995. Absence of geographic chromosomal variation in the roan and sable antelope and the cytogenetics of a naturally occurring hybrid. *Cytogenet Cell Genet.* **71**:363–369.
- Sánchez-Barreiro F, Gopalakrishnan S, Ramos-Madrigal J, Westbury MV, de Manuel M, Margaryan A, Ciucani MM, Vieira FG, Patramanis Y, Kalthoff DC, et al. 2021. Historical population declines prompted significant genomic erosion in the northern and southern white rhinoceros (*Ceratotherium simum*). *Mol Ecol.* **30**: 6355–6369.
- Skead CJ. 1980. Blue antelope (extinct blaauwbok), *Hippotragus leucophaeus* (Pallas, 1766). In: *Historical mammal incidence in the Cape Province*. Vol. 1. 2nd ed. Cape Town: Department of Nature and Environmental Conservation of the Provincial Administration of the Cape of Good Hope. p. 526–537.
- Skead CJ. 2011. *Historical incidence of the larger land mammals in the broader western and northern Cape*. Port Elizabeth: Centre for African Conservation Ecology, Nelson Mandela Metropolitan University.
- Skoglund P, Thompson JC, Prendergast ME, Mittnik A, Sirak K, Hajdinjak M, Salie T, Rohland N, Mallick S, Peltzer A, et al. 2017. Reconstructing prehistoric African population structure. *Cell* **171**:59–71.e21.
- Smith A. 1849. *Illustrations of the zoology of South Africa*. London: Smith, Elder and Co.
- Smith CI, Chamberlain AT, Riley MS, Cooper A, Stringer CB, Collins MJ. 2001. Not just old but old and cold? *Nature* **410**:771–772.
- Stamatakis A. 2014. RAxML version 8: a tool for phylogenetic analysis and post-analysis of large phylogenies. *Bioinformatics* **30**:1312–1313.
- Stuiver M, Reimer PJ. 1993. Extended ^{14}C data base and revised CALIB 3.0 ^{14}C age calibration program. *Radiocarbon* **35**:215–230.
- Themudo GE, Campos PF. 2018. Phylogenetic position of the extinct blue antelope, *Hippotragus leucophaeus* (Pallas, 1766) (Bovidae: Hippotraginae), based on complete mitochondrial genomes. *Zool J Linn Soc.* **182**:225–235.
- van Andel TH. 1989. Late Pleistocene sea levels and the human exploitation of the shore and shelf of southern South Africa. *J Field Archaeol.* **16**:133–155.
- Vankan M, Ho SYW, Duchêne DA. 2022. Evolutionary rate variation among lineages in gene trees has a negative impact on species-tree inference. *Syst Biol.* **71**:490–500.
- Vaz Pinto P, Beja P, Ferrand N, Godinho R. 2016. Hybridization following population collapse in a critically endangered antelope. *Sci Rep.* **6**:18788.
- Venter JA, Brooke CF, Marean CW, Fritz H, Helm CW. 2020. Large mammals of the Palaeo-Agulhas Plain showed resilience to extreme climate change but vulnerability to modern human impacts. *Quat Sci Rev.* **235**:106050.
- Vicente M, Schlebusch CM. 2020. African population history: an ancient DNA perspective. *Curr Opin Genet Dev.* **62**:8–15.
- von Schreber JCD, Goldfuß A. 1836. Die Säugthiere in Abbildungen nach der Natur mit Beschreibungen. Erlangen.
- Vrba ES, Gatesy J. 1994. New antelope fossils from Awash, Ethiopia, and phylogenetic analysis of Hippotragini (Bovidae, Mammalia). *Palaeont Afr.* **31**:55–72.
- Wadley L. 1993. The Pleistocene Later Stone Age south of the Limpopo River. *J World Prehist.* **7**:243–296.
- Westbury MV, Hartmann S, Barlow A, Preick M, Ridush B, Nagel D, Rathgeber T, Ziegler R, Baryshnikov G, Sheng G, et al. 2020. Hyena paleogenomes reveal a complex evolutionary history of cross-continental gene flow between spotted and cave hyena. *Sci Adv.* **6**:eaay0456.
- Westbury MV, Hartmann S, Barlow A, Wiesel I, Leo V, Welch R, Parker DM, Sicks F, Ludwig A, Dalén L, et al. 2018. Extended and continuous decline in effective population size results in low genomic diversity in the world's rarest hyena species, the brown hyena. *Mol Biol Evol.* **35**:1225–1237.
- Xue Y, Prado-Martinez J, Sudmant PH, Narasimhan V, Ayub Q, Szpak M, Frandsen P, Chen Y, Yngvadottir B, Cooper DN, et al. 2015. Mountain gorilla genomes reveal the impact of long-term population decline and inbreeding. *Science* **348**:242–245.